DRUG DISCOVERY

Author Affiliation:
[1]Department of Natural Sciences, Northeastern State University, Broken Arrow, Oklahoma 74014, The United States of America

[*]Corresponding author
Department of Natural Sciences, Northeastern State University,
Broken Arrow, Oklahoma 74014,
USA
Email: kim03@nsuok.edu
ORCID: orcid.org/0000-0002-2325-245X

DISCOVERY
SCIENTIFIC SOCIETY

Inhibition of New Delhi Metallo-β-lactamase 1 from *Klebsiella pneumoniae* by an L-aspartic acid derivative

Destiny Morris M[1], Jhawn Saul G[1], Sarah Faubion C[1], Kaliana Lee C[1], Sung-Kun Kim[1*]

ABSTRACT

The overuse of β-lactam antibiotics has caused drug-resistant bacteria, including NDM-1, a Metallo-β-lactamase that renders inhibitors ineffective. NDM-1 is found in *Klebsiella pneumoniae*, causing worldwide resistant infections. Developing an NDM-1 inhibitor is vital for managing bacterial resistance and public health. This study investigated L-aspartic acid β-benzyl ester 7-amido-4-methylcoumarin (Asp (OBzl)-AMC) as a potential NDM-1 inhibitor through in vitro and in silico evaluations. Enzyme kinetics indicated competitive inhibition, with an IC_{50} value of 30.4 ± 5.0 μM and a K_i value of 11.4 ± 1.2 μM. Molecular docking showed Asp (OBzl)-AMC forming hydrogen bonds with NDM-1's active site residues. Asp (OBzl)-AMC displayed favorable ADME properties, making it a promising drug candidate. The study demonstrates that Asp (OBzl)-AMC effectively binds to NDM-1 and inhibits its activity. The compound's attachment to the naphthalene ring is crucial for protecting β-lactam antibiotics from NDM-1 damage. These findings suggest that Asp (OBzl)-AMC holds potential as an NDM-1 inhibitor to combat bacterial resistance and maintain public health.

Keywords: Metallo-beta-lactamase, enzyme, inhibition, kinetics, molecular dynamics

1. INTRODUCTION

Inhibition of bacterial infections is essential for maintaining human health (Al-Jalali and Zeitlinger, 2018; Shamriz and Shoenfeld, 2018). β-lactam antibiotics, including penicillins, carbapenems, and cephalosporins, are widely employed to treat such infections (Edwards, 2000; Essack, 2001; Liu et al., 2018; Paterson et al., 2001). However, excessive use of these antibiotics has led to the emergence of drug-resistant bacteria, resulting in a decline in the efficacy of these drugs and raising concern for public health (Khan-Ali et al., 2017; Khan-Maryam et al., 2017). The primary cause of antibiotic resistance is the proliferation of β-lactamases, enzymes that catalyze the hydrolysis of β-lactam antibiotics. These enzymes are classified into four classes, A through D, with class B requiring zinc ions in the

active site for activity, and are referred to as metallo-β-lactamases (MBLs) (Hawk et al., 2009).

The subclass B of Metallo-β-lactamases (MBLs) is further classified into three subcategories: B1, B2, and B3. Currently, β-lactamase inhibitors, including clavulanic acid, sulbactam, and tazobactam, are commercially available and can be used in conjunction with antibiotics to treat some antibiotic-resistant infections, but all are ineffective against MBLs. Despite the presence of potential inhibitors for MBLs (Crowder et al., 2006; Materon et al., 2003), none are commercially available for use against these enzymes. Given the prolonged drug development process, it is imperative to identify effective inhibitors for MBLs.

A strain of *Klebsiella pneumoniae* emerging from India has been found to produce an MBL of the B1 subclass, known as New Delhi Metallo-β-lactamase-1 (NDM-1) (Brem et al., 2016; Groundwater et al., 2016). This enzyme contains two zinc ions, Zn1 and Zn2, which are directly involved in its catalytic function. The presence of NDM-1 has since been reported in various regions worldwide (Heinz et al., 2019; Johnson and Woodford, 2013; Tran et al., 2015). NDM-1's resistance to β-lactamase inhibitors is primarily due to its ability to hydrolyze the amide bond of the β-lactam ring (King et al., 2012). The resistance of pathogenic bacteria to treatment presents a significant challenge to disease management (Ejaz et al., 2020). As such, targeting NDM-1 may potentially inhibit the resistance of pathogenic bacteria.

Genes associated with NDM-1 can be transferred to *Escherichia coli* (Shah et al., 2015; Tuem et al., 2018; Zhang et al., 2017). In recent years, resistance to *E. coli* has increased among the population (Wang et al., 2015). NDM-1 plays a significant role in those bacterial resistance mechanisms (Du et al., 2017). Plasmids containing NDM-1 in patients can spread among different species of Enterobacteriaceae, another common pathogenic bacteria in healthcare settings (Martino et al., 2019). Bacterial infections resulting in this type of resistance to antibiotics not only increase medical expenses but also poses a threat to human health (Yang et al., 2017).

Therefore, it is of paramount importance to develop an effective drug that can inhibit NDM-1. In this study, we aimed to investigate the potential of L-aspartic acid β-benzyl ester 7-amido-4-methylcoumarin (hereafter referred to as Asp (OBzl)-AMC) as an NDM-1 inhibitor, given its possession of a potential zinc-binding group, ester and amide. The ability of the compound to effectively bind the zinc ion in the active site was evaluated using both *in vitro* and *in silico* methods. Enzyme kinetics inhibition studies and a series of molecular dynamics simulations of NDM-1 in complex with the compound Asp (OBzl)-AMC were conducted. These results may offer a promising approach for developing a potential drug that targets NDM-1.

2. MATERIALS AND METHODS

General Procedures

All chemicals were obtained through Sigma or other quality manufacturers. The NDM-1 gene from *K. pneumoniae* was inserted into the pET100 vector using the Champion pET Directional TOPO Expression Kit from Invitrogen (Waltham, MA, USA). The enzyme was purified using previously established methods with the pET100-NDM-1 construct (Schlesinger et al., 2011). The product's purity was determined through Ni^{2+} chromatography using 10% SDS-PAGE. Additional purification was achieved through gel-filtration chromatography if necessary. The enzyme was stored at -20°C in 50 mM 3-(N-morpholino) propane sulfonic acid (MOPS) (pH 7.0), 0.050mM ZnSO4, and 30% (v/v) glycerol for further experimentation when it was determined to be 95% pure or higher. Asp (OBzl)-AMC was used as a substrate and was prepared by dissolving it in dimethyl sulfoxide (DMSO) before being diluted to various concentrations for enzyme activity assays.

Inhibition Tests

The purified NDM-1 enzyme activity was assessed by adding it to solutions of nitrocefin (ranging from 10 to 70 μM) in 50 mM MOPS (pH 7.0) at a final concentration of 0.13 μg/mL, in a total volume of 1 mL, using quartz cuvettes at room temperature. The increase in absorbance at 485 nm resulting from the hydrolysis of nitrocefin ($\varepsilon = 15,900$ $M^{-1} \cdot cm^{-1}$) was used as a measure of enzyme activity, and the assays were conducted in triplicate (Fast et al., 2001). The IC_{50}, or the concentration of inhibitor required to inhibit 50% of enzymatic activity, was determined using an enzyme assay with Asp (OBzl)-AMC as the inhibitor and nitrocefin as the substrate. The assay was performed using a fixed concentration of nitrocefin (0.4 mM) and a fixed enzyme concentration (0.13 μg/mL or 4.8 nM) after a 1-minute incubation period with varying inhibitor concentrations. To further analyze the mode of inhibition, a separate series of assays were conducted at fixed inhibitor concentrations (0 – 0.030 mM) with varying substrate concentrations (0.1 to 0.4 mM) and analyzed using Lineweaver-Burk plots and non-linear regression through Sigma Plot version 11.0. The competitive inhibition equation, $v = V_{max} \cdot S/[K_m \cdot (1 + 1/K_i) + S]$, was used for data analysis. All experiments were performed in triplicate.

Molecular Docking Simulations

This study used the crystal structure of the Metallo-β-lactamase NDM-1 (PDB id: 4EY2) as a starting point. The structure of Asp (OBzl)-AMC was computationally generated using the Avogadro program, with energy minimization carried out using the General Amber Force Fields (Hanwell et al., 2012). A molecular docking simulation was performed for each ligand using the Autodock Vina program, with full flexibility for the ligand and a rigid receptor. The active site of NDM-1 was defined as the center of a grid box with dimensions of 45 Å x 45 Å x 45 Å, with the x-y-z coordinates of (-0.509, 8.133, 23.576). The lowest energy docking results for each ligand were used for further analysis through molecular dynamics. The Protein-Ligand Interaction Profiler (PLIP) online server was utilized to analyze the interactions from the Autodock results and the final conformations obtained from molecular dynamics (Adasme et al., 2021).

Molecular Dynamics Simulations

All molecular dynamics simulations were conducted using the Gromacs program version 2021.4. The AMBER99SB-ILDN force field, modified with recently published zinc (II)-binding residues parameters, was employed in these simulations (Macchiagodena et al., 2019; Macchiagodena et al., 2020). The modifications to the force field were implemented to ensure accurate coordination of the active site zinc ions, thereby enhancing the stability of the metalloprotein during the dynamics simulation. The SPC/E water model was used in the simulation. To create the topologies of the ligands for use in Gromacs, the Acpype program was utilized (Sousa-da-Silva and Vranken, 2012). The initial step of each dynamics simulation involved solvating the system and neutralizing it by adding three chlorine ions. An energy minimization was then performed for 50,000 steps using the steepest descent algorithm. The system was equilibrated in two phases: A 100 ps run using the NVT ensemble with the leap-frog integrator, which stabilized the temperature at 300 K, and a 100 ps run using the NPT ensemble with the leap-frog integrator, which stabilized the pressure at 1 bar.

Position restraints were applied to the receptor and ligand during each equilibration run. The Berendsen V-rescale thermostat was used to regulate the temperature, and the Parrinello-Rahman barostat was used to regulate the pressure. The final production MD simulation was run for 100 ns, with the position restraints removed. Two replicate simulations were conducted for the NDM-1: Asp (OBzl)-AMC complex system with different initial velocities and were compared to identify consistent behavior. The replicate with the best fit was then used to further analyze and compare inhibitors. The root-mean-square deviation (RMSD) of each inhibitor trajectory relative to the protein backbone was calculated using the RMSD module of Gromacs. Additionally, the protein backbone RMSD relative to the energy-minimized conformation was calculated for each system to provide insight into the protein stability throughout the simulations.

Free Energy Calculations

Each simulation's average end-state free energy was calculated using the molecular mechanics with the generalized Born and surface area (MM-GBSA) model implemented in the gmx_MMPBSA program (Valdés-Tresanco et al., 2021). To perform this calculation, 100 snapshots were taken from each simulation. The binding free energy and a per-residue decomposition of the free energy were calculated according to a previously published method (Huckleby et al., 2022).

3. RESULTS

IC$_{50}$ value determination

To investigate the potential inhibitory effect of Asp (OBzl)-AMC on NDM-1 activity, we conducted an assay to determine its IC$_{50}$ values. Various Asp (OBzl)-AMC concentrations, ranging from 0.5 μM to 100 mM, were used to obtain the IC$_{50}$ values. The obtained data were analyzed using the concentration-response equation $v_i/v_o = 1/(1 + ([I]/IC_{50})^h)$, where I denote the inhibitor and h is the Hill coefficient (values of h were between 0.5 and 1). The data points of Asp (OBzl)-AMC exhibited a satisfactory fit to a semilogarithmic concentration-response plot, as demonstrated in Figure 1. By calculating the IC$_{50}$ value at 50% inhibition, we determined that the IC$_{50}$ of Asp (OBzl)-AMC was 30.4 ± 5.0 μM.
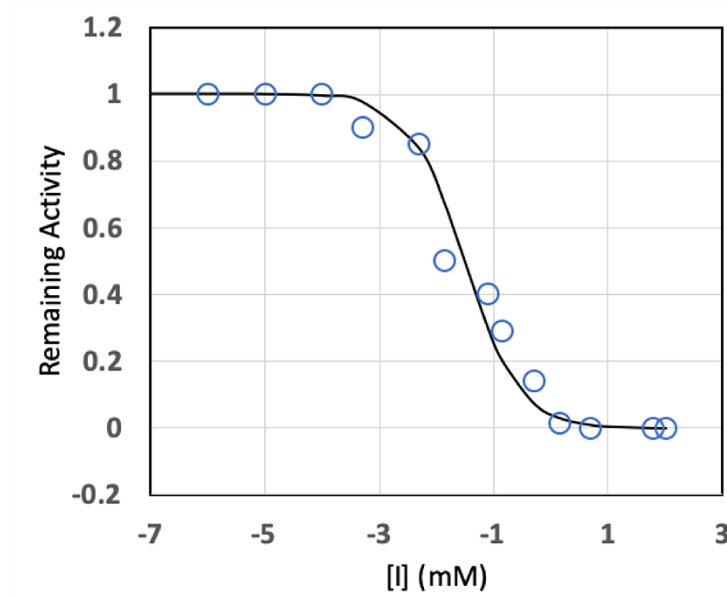
Figure 1 Concentration-response plots for the inhibition of NDM-1 by Asp (OBzl)-AMC. The letter I denote the inhibitor Asp (OBzl)-AMC. The data points are based on the average values obtained from triplicate analysis.

Mode of inhibition assay

To investigate the mode of inhibition, inhibitory enzyme assays were performed using varying concentrations of the substrate cephalexin and Asp (OBzl)-AMC. The Lineweaver-Burk plots for Asp (OBzl)-AMC are presented in Figure 2, demonstrating an intersection of lines at the y-axis. The K_i values were calculated from the slopes of the plots, resulting in a K_i value of 11.4 ± 1.2 μM. The apparent K_m values were determined from Figure 2 to calculate the K_i values.
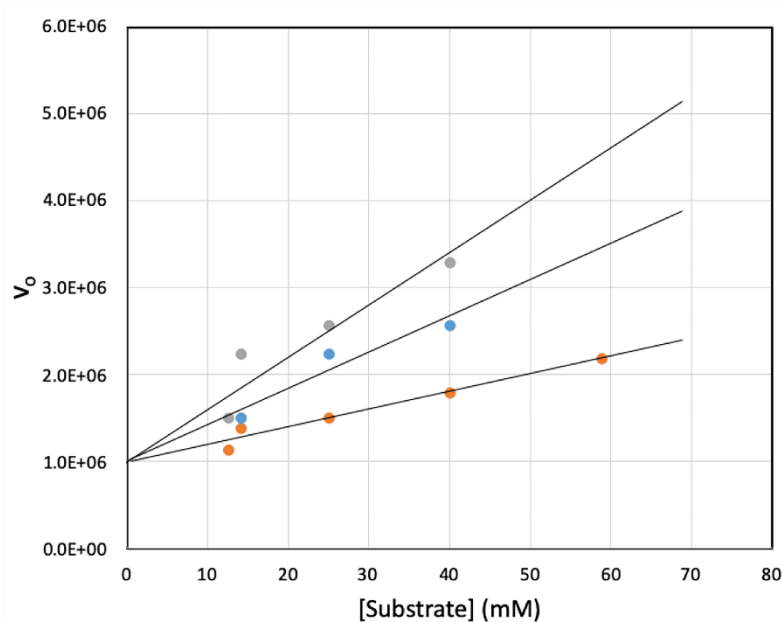

Figure 2 Lineweaver-Burk plots of the inhibition of NDM-1 by Asp (OBzl)-AMC. Cephalexin was used as the substrate. The assays were carried out in a buffer of 50 mM MOPS at pH 7.0. Kinetic constants were determined by fitting the data to the equation $v = V_{max} \cdot S/(K_m \cdot (1 + 1/K_i) + S)$, which indicates competitive inhibition. The concentrations of the inhibitor Asp (OBzl)-AMC used were 0 (orange), 20 (blue), and 40 μM (gray). All data points are based on the average values obtained from triplicate analysis.

Molecular docking simulations

Molecular docking simulations were employed to simulate the possible inhibition of NDM-1 by Asp (OBzl)-AMC. The complex with the lowest energy and a ΔG value of -7.8 kcal/mol was selected for further dynamics analysis. The conformation of the chosen

complex demonstrated that the carboxyl group interacts with a Zn (II) ion, while a potential hydrogen bond was observed between the compound and active site residues His249, as illustrated in Figure 3.
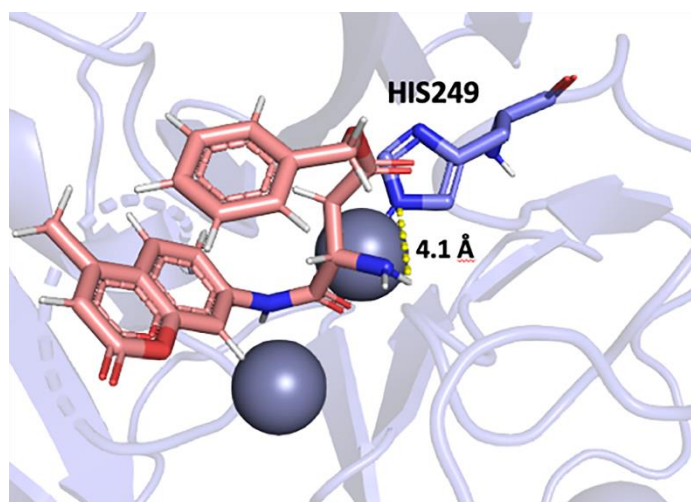

Figure 3 Autodock binding conformation selected for dynamics. The compound Asp (OBzl)-AMC was centered in pink color. The oxygen element was colored in red and other elements were colored in purple or dark purple.

We employed a PLIP to comprehensively analyze the protein-inhibitor interaction. The results, depicted in Figure 4, reveal the occurrence of hydrophobic, hydrogen bonding, and salt bridge interactions between the inhibitor and NDM-1. A detailed account of the chemical interactions can be found in Table 1.
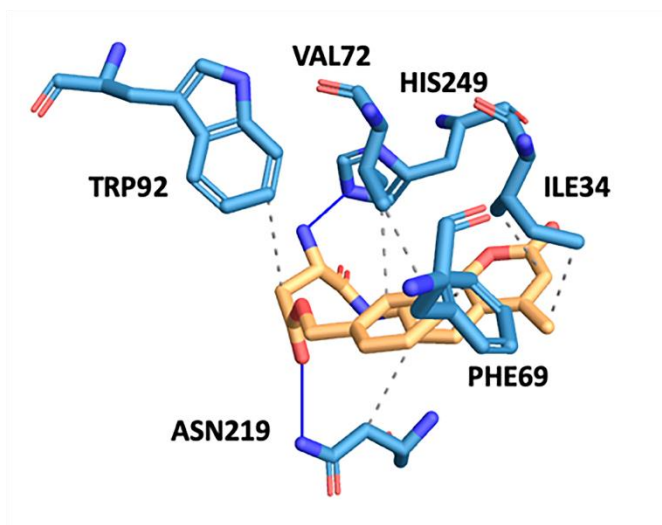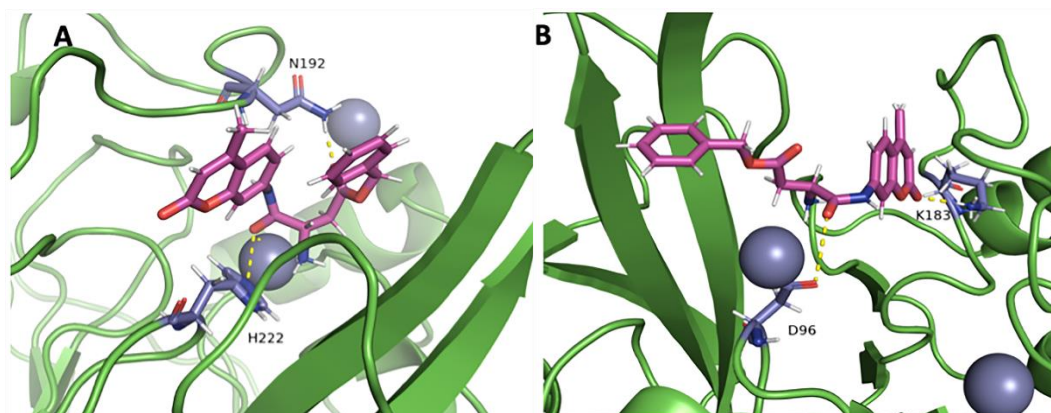

Figure 4 Evaluating docking results with PLIP. The protein is depicted in red, the inhibitor in orange, and the charge center in yellow. Hydrophobic interactions are shown by gray dashed lines and hydrogen bonds by purple solid lines.

A 100 ns molecular dynamics simulation was conducted to investigate the molecular interactions between the ligand and receptor in the context of hydration. The lowest energy docking result was used to initiate the simulation, which resulted in a ΔG value of -7.8 kcal/mol. Although the initial molecular docking suggested a hydrogen bond between His249 and the ligand, the molecular dynamics simulation showed that Asn192 and His222 also formed hydrogen bonds due to equilibrium processes. The simulation snapshots captured in Figure 5 revealed the hydrogen interactions at various stages of the simulation, including between the naphthalene ring of the inhibitor and the epsilon-amino group of Lys183, as well as between the naphthalene ring of the inhibitor and the carbonyl oxygen of the peptide of Leu190. These observations suggest that the naphthalene ring moiety of the inhibitor is critical for its interaction with the target enzyme.

Table 1 The non-covalent interactions (hydrogen bonds and hydrophobic interactions) between the inhibitor and the enzyme.

Hydrogen Bonds							
Index	Residue	AA	Distance H-A	Distance D-A	Donor Angle	Protein Donor	Side Chain
1	219	Asn	2.06	3.06	173.57	✓	✓
2	249	His	2.26	2.86	116.50	x	✓
Hydrophobic Interactions							
Index		Residue		AA		Distance	
1		34		Ile		3.52	
2		34		Ile		3.50	
3		69		Phe		3.22	
4		72		Val		3.83	
5		72		Val		3.98	
6		92		Trp		3.79	
7		219		Asn		3.90	

The RMSD values for the atomic positions obtained from the simulation were analyzed to examine conformational binding variations in a hydrated environment (Figure 6). The RMSD of the peptide backbone of the enzyme remained stable after 0.7 ns, indicating that the molecular system was well-behaved throughout the simulation. Similarly, the RMSD of the inhibitor atoms stabilized after 0.2 ns, indicating that the system was well-equilibrated.

Figure 5 Snapshots of the molecular dynamics simulation for Asp (OBzl)-AMC with NDM-1 at the beginning of the simulation (A) and 75 ns (B).

To gain a more detailed understanding of the interactions between NDM-1 and Asp (OBzl)-AMC, the decomposition data for the system were analyzed (Figure 7). The MM-GBSA technique was employed to determine the binding free energy of Asp (OBzl)-AMC in complex with NDM-1, with a ΔG binding value of -21.78 kcal/mol estimated based on the inhibitor confirmation obtained from the molecular dynamics simulation.

Pharmacokinetics properties

The pharmacokinetics properties of a lead compound, commonly referred to as Absorption, Distribution, Metabolism, and Excretion (ADME), are crucial for a drug's success. These parameters track the drug's behavior in the body from administration to excretion through sweat, urine, or feces (Dowty et al., 2010). The distribution volume to tissues and target sites affects the drug's bioavailability and minimizes side and toxic effects. Evaluating a drug candidate's efficacy and toxicity before clinical trials can reduce the risk of unwanted effects in human or animal models. The online Swiss ADME server can assist in reducing costs by predicting potential drug rejection. Our study evaluated the ADME properties, including lipophilicity, water-solubility, drug-likeness, and medicinal chemistry, of Asp (OBzl)-AMC. The ADME properties of Asp (OBzl)-AMC were found to be in an optimal range, as listed in Table 2.
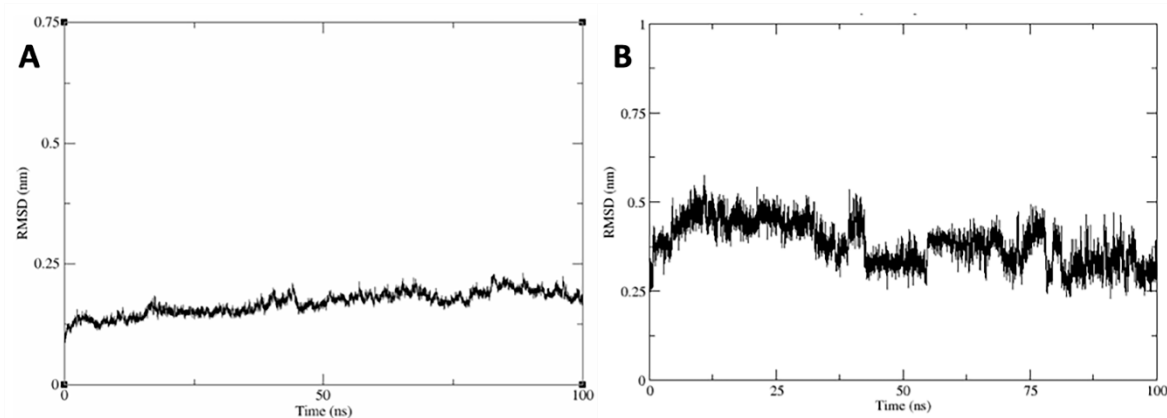
Figure 6 The RMSDs for the complexes and the compounds. (A) NDM-1 backbone RMSD from the NDM-1: Asp (OBzl)-AMC complex (B) RMSD of Asp (OBzl)-AMC from the NDM-1: Asp (OBzl)-AMC complex. Plotted as running averages for visual clarity.
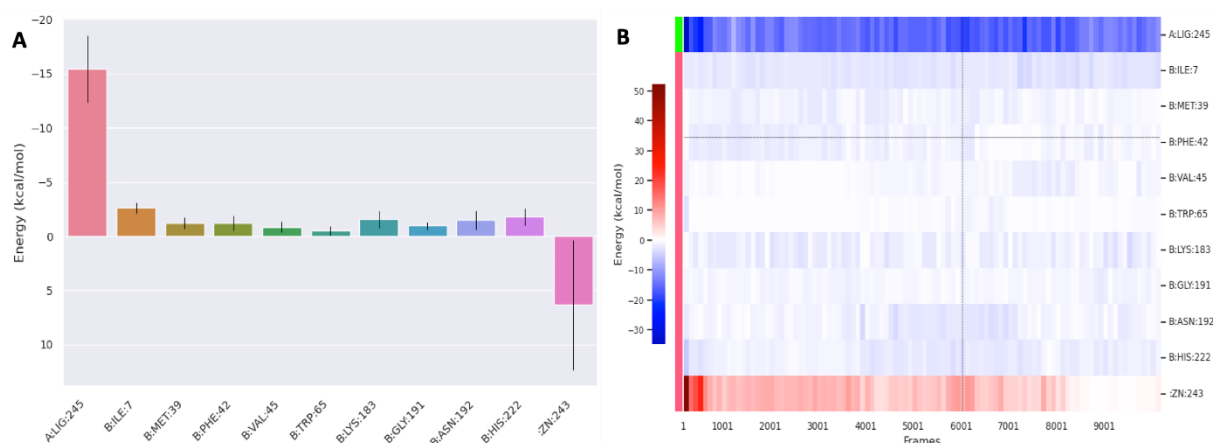

Figure 7 Per-residue energy decomposition diagrams. (A) Binding free energy decomposition of the NDM-1: Asp (OBzl)-AMC complex, (B) Per-residue energy decomposition heatmap.

Table 2 Identification of Physical, Chemical, Pharmacokinetic, and Drug-Likeness Properties of Asp (OBzl)-AMC.

Properties	Parameter	Asp (OBzl)-AMC
Physicochemical properties	MW (g/mol)	290.27 g/mol
	Num. heavy atoms	21
	Num. arom. heavy atoms	10
	Num. rotatable bonds	5
	Num. hydrogen bond acceptors	6
	Num. hydrogen bond donors	3
	Molar refractivity	75.86
Lipophilicity	Log $P_{o/w}$	0.58
Water solubility	Log S (ESOL)	-0.61
Pharmacokinetics	GI absorption	High
	Blood-Brain Barrier permeant	No
	CYP3A4 inhibitor	No
Drug likeness	Lipinski violation	0 violation
	Bioavailability score	0.55
Medi. chemistry	Synthetic accessibility	3.17

4. DISCUSSION

We have demonstrated the potential for inhibition of NDM-1 by an L-aspartic acid derivative that can bind to the zinc ion in the active site. The effectiveness of the zinc ion binding was investigated by way of *in silico* and *in vitro* analyses. The MD simulations of NDM-1 in complex with the L-aspartic acid derivative revealed the details of the binding interactions. In addition, kinetic analyses were performed to examine the inhibitory potential of each compound. The performance of the MD simulations for the NDM-1: Asp (OBzl)-AMC complex clearly showed the ability of the L-aspartic acid derivative to remain bound to the zinc in the active site. The naphthalene ring moiety of Asp (OBzl)-AMC appears to confer unique advantages in interacting with the Lys183 and Leu190 side chains in various ways. Also, according to PLIP and per-residue decomposition data obtained from MD simulations, the hydrophobic interactions around the aromatic ends of Asp (OBzl)-AMC contributed significantly to stabilizing the compound within the NDM-1 active site.

Furthermore, it should be mentioned here that the molecular docking results appeared to be adjusted for the beginning of the molecular dynamics simulation, as the target enzyme is rigid in Auto Dock, while the latter offers total flexibility for the complex. The experimental and in silico inhibition studies suggest that the inhibition mode is likely to be competitive. These compounds bind strongly to the active site zinc ions, as evidenced by the MD simulations, reaffirming their potential as competitive inhibitors. Moreover, the IC_{50} and K_i values were in the low micromolar range. Given all these findings, Asp (OBzl)-AMC could serve as a promising drug candidate and a lead compound for further development. Structural modifications can be made to enhance the drug's effectiveness, and a structure-activity relationship analysis should be conducted. It is also crucial to evaluate the cytotoxicity and specificity of these compounds before using them in clinical settings.

5. CONCLUSION

To summarize, we have created an L-aspartic acid derivative with a strong affinity for NDM-1, a major contributor to β-lactam antibiotic resistance. The compound has demonstrated potential for inhibiting NDM-1, with IC_{50} values in the micromolar range and a K_i value in the low micromolar range indicating strong binding. Molecular dynamics simulations have provided insight into the specific amino acids involved in the complex formation between Asp (OBzl)-AMC and NDM-1. The experimental inhibition studies have supported the idea that the mode of inhibition is competitive, which aligns with data obtained from *in silico* analysis. The attachment of the L-aspartic acid derivative to the naphthalene ring is believed to be crucial for interaction with zinc ions, contributing to the compound's effectiveness in inhibiting NDM-1. We anticipate that this compound will protect β-lactam antibiotics from the damage caused by NDM-1.

Author Contributions

Data curation: DMM, JGS, SCF, KCL and SKK; Formal analysis: DMM, JGS, SCF and SKK; Funding acquisition: SKK; Writing– original draft: DMM, JGS and SKK; Writing–review & editing: DMM, JGS, SCF, KCL and SKK. All authors have read and agreed to the published version of the manuscript.

Informed consent

Not applicable.

Ethical approval

Not applicable.

Conflicts of interests

The authors declare that there are no conflicts of interests.

Data and materials availability

All data associated with this study are present in the paper.

REFERENCES AND NOTES

1. Adasme MF, Linnemann KL, Bolz SN, Kaiser F, Salentin S, Haupt VJ, Schroeder M. PLIP 2021: Expanding the scope of the protein–ligand interaction profiler to DNA and RNA. Nucleic Acids Res 2021; 49(W1):530–W534.

2. Al-Jalali V, Zeitlinger M. Clinical Pharmacokinetics and Pharmacodynamics of Telavancin Compared with the Other Glycopeptides. Clin Pharmacokinet 2018; 57(7):797–816.

3. Brem J, Berkel SSV, Zollman D, Lee SY, Gileadi O, McHugh PJ, Walsh TR, McDonough MA, Schofield CJ. Structural Basis of Metallo-β-Lactamase Inhibition by Captopril Stereoisomers. Antimicrob Agents Chemother 2016; 60(1):42–150.

4. Crowder MW, Spencer J, Vila AJ. Metallo-β-lactamases: Novel Weaponry for Antibiotic Resistance in Bacteria. Acc Chem Res 2006; 39(10):721–728.

5. Dowty ME, Messing DM, Lai Y, Kirkovsky L. Adme. ADMET Med Chem 2010; 145-200.

6. Du J, Li B, Cao J, Wu Q, Chen H, Hou Y, Zhang E, Zhou T. Molecular Characterization and Epidemiologic Study of NDM-1-Producing Extensively Drug-Resistant Escherichia coli. Microb Drug Resist 2017; 23(3):272–279.

7. Edwards JR. Carbapenems: The pinnacle of the beta-lactam antibiotics or room for improvement? J Antimicrob Chemother 2000; 45(1):1–4.

8. Ejaz H, Alzahrani B, Hamad MFS, Abosalif KOA, Junaid K, Abdalla A, Elamir MYM, Aljaber N, Hamam SSM, Younas S. Molecular Analysis of the Antibiotic Resistant NDM-1 Gene in Clinical Isolates of Enterobacteriaceae. Clin Lab 2020; 66(3). doi: 10.7754/clin.lab.2019.190727.

9. Essack SY. The development of beta-lactam antibiotics in response to the evolution of beta-lactamases. Pharm Res 2001; 18(10):1391–1399.

10. Fast W, Wang Z, Benkovic SJ. Familial Mutations and Zinc Stoichiometry Determine the Rate-Limiting Step of Nitrocefin Hydrolysis by Metallo-β-lactamase from Bacteroides fragilis. Biochem 2001; 40(6):1640–1650.

11. Groundwater PW, Xu S, Lai F, Váradi L, Tan J, Perry JD, Hibbs DE. New Delhi metallo-β-lactamase-1: Structure, inhibitors and detection of producers. Future Med Chem 2016; 8(9):993–1012.

12. Hanwell MD, Curtis DE, Lonie DC, Vandermeersch T, Zurek E, Hutchison GR. Avogadro: An advanced semantic chemical editor, visualization, and analysis platform. J Cheminf 2012; 4 (1):17.

13. Hawk MJ, Breece RM, Hajdin CE, Bender KM, Hu Z, Costello AL, Bennett B, Tierney DL, Crowder MW. Differential Binding of Co(II) and Zn(II) to Metallo-β-Lactamase Bla2 from Bacillus anthracis. J Am Chem Soc 2009; 131(30):10753–10762.

14. Heinz E, Ejaz H, Bartholdson-Scott J, Wang N, Gujaran S, Pickard D, Wilksch J, Cao H, Haq I, Dougan G, Strugnell RA. Resistance mechanisms and population structure of highly drug resistant Klebsiella in Pakistan during the introduction of the carbapenemase NDM-1. Sci Rep 2019; 9(1):2392.

15. Huckleby AE, Saul JG, Shin H, Desmarais S, Bokka A, Jeon J, Kim SK. Development of Hydroxamic Acid Compounds for Inhibition of Metallo-β-Lactamase from Bacillus anthracis. Int J Mol Sci 2022; 23(16):9163.

16. Johnson AP, Woodford N. Global spread of antibiotic resistance: The example of New Delhi metallo-β-lactamase (NDM)-mediated carbapenem resistance. Int J Med Microbiol 2013; 62(4):499–513.

17. Khan AU, Ali A, Danishuddin, Srivastava G, Sharma A. Potential inhibitors designed against NDM-1 type metallo-β-lactamases: an attempt to enhance efficacies of antibiotics against multi-drug-resistant bacteria. Sci Rep 2017; 7(1):9207.

18. Khan AU, Maryam L, Zarrilli R. Structure, Genetics and Worldwide Spread of New Delhi Metallo-β-lactamase (NDM): a threat to public health. BMC Microbiol 2017; 17(1):101.

19. King DT, Worrall LJ, Gruninger R, Strynadka NCJ. New Delhi Metallo-β-Lactamase: Structural Insights into β-Lactam Recognition and Inhibition. J Am Chem Soc 2012; 134(28):113 62–11365.

20. Liu S, Jing L, Yu ZJ, Wu C, Zheng Y, Zhang E, Chen Q, Yu Y, Guo L, Wu Y, Li GB. ((S)-3-Mercapto-2-methylpropanamido) acetic acid derivatives as metallo-β-lactamase inhibitors: Synthesis, kinetic and crystallographic studies. Eur J Med Chem 2018; 145:649–660.

21. Macchiagodena M, Pagliai M, Andreini C, Rosato A, Procacci P. Upgraded AMBER Force Field for Zinc-Binding Residues and Ligands for Predicting Structural Properties and Binding Affinities in Zinc-Proteins. ACS Omega 2020; 5(25):15301–153 10.

22. Macchiagodena M, Pagliai M, Andreini C, Rosato A, Procacci P. Upgrading and Validation of the AMBER Force Field for Histidine and Cysteine Zinc(II)-Binding Residues in Sites with Four Protein Ligands. J Chem Inf Model 2019; 59(9):3803–381 6.

23. Martino F, Tijet N, Melano R, Petroni A, Heinz E, De-Belder D, Faccone D, Rapoport M, Biondi E, Rodrigo V, Vazquez M, Pasteran F, Thomson NR, Corso A, Gomez SA. Isolation of five Enterobacteriaceae species harbouring blaNDM-1 and

mcr-1 plasmids from a single paediatric patient. PloS one 2019; 14(9):e0221960.

24. Materon IC, Queenan AM, Koehler TM, Bush K, Palzkill T. Biochemical Characterization of β-Lactamases Bla1 and Bla2 from Bacillus anthracis. Antimicrob Agents Chemother 2003; 47(6):2040–2042.

25. Paterson DL, Ko WC, Von-Gottberg A, Casellas JM, Mulazimoglu L, Klugman KP, Bonomo RA, Rice LB, McCormack JG, Yu VL. Outcome of Cephalosporin Treatment for Serious Infections Due to Apparently Susceptible Organisms Producing Extended-Spectrum β-Lactamases: Implications for the Clinical Microbiology Laboratory. J Clin Microbiol 2001; 39(6):2206–2212.

26. Schlesinger SR, Kim SG, Lee JS, Kim SK. Purification development and characterization of the zinc-dependent metallo-β-lactamase from Bacillus anthracis. Biotechnol Lett 2011; 33(7):417-1422.

27. Shah MS, Eppinger M, Ahmed S, Shah AA, Hameed A, Hasan F. Multidrug-resistant diarrheagenic E coli pathotypes are associated with ready-to-eat salad and vegetables in Pakistan. J Korean Soc Appl Biol Chem 2015; 58(2):267–273.

28. Shamriz O, Shoenfeld Y. Infections: a double-edge sword in autoimmunity. Current Opinion in Rheumatology 2018; 30(4): 365–372.

29. Sousa-da-Silva AW, Vranken WF. ACPYPE - AnteChamber PYthon Parser interface. BMC Res Notes 2012; 5(1):367.

30. Tran HH, Ehsani S, Shibayama K, Matsui M, Suzuki S, Nguyen MB, Tran DN, Tran VP, Tran DL, Nguyen HT, Dang DA, Trinh HS, Nguyen TH, Wertheim HFL. Common isolation of New Delhi metallo-beta-lactamase 1-producing Enterobacteriaceae in a large surgical hospital in Vietnam. Eur J Clin Microbiol Infect Dis 2015; 34(6):1247–1254.

31. Tuem KB, Gebre AK, Atey TM, Bitew H, Yimer EM, Berhe DF. Drug Resistance Patterns of Escherichia coli in Ethiopia: A Meta-Analysis. Biomed Res Int 2018; 1–13.

32. Valdés-Tresanco MS, Valdés-Tresanco ME, Valiente PA, Moreno E. gmx_MMPBSA: A New Tool to Perform End-State Free Energy Calculations with GROMACS. J Chem Theory Comput 2021; 17(10):6281–6291.

33. Wang X, Lu M, Shi Y, Ou Y, Cheng X. Discovery of Novel New Delhi Metallo-β-Lactamases-1 Inhibitors by Multistep Virtual Screening. PLoS One 2015; 10(3):e0118290.

34. Yang SC, Lin CH, Aljuffali IA, Fang JY. Current pathogenic Escherichia coli foodborne outbreak cases and therapy development. Arch Microbiol 2017; 199(6):811–825.

35. Zhang J, Wang S, Wei Q, Guo Q, Bai Y, Yang S, Song F, Zhang L, Lei X. Synthesis and biological evaluation of Aspergillomarasmine A derivatives as novel NDM-1 inhibitor to overcome antibiotics resistance. Bioorg Med Chem 2017; 25 (19):5133–5141.